Research project report: Modelling MAPK/ERK pathway using Ordinary Differential Equations

Przemysław Pilipczuk

A mechanistic model of MAPK/ERK signaling pathway was constructed using Ordinary Differential Equations and implemented into a pipeline for simulating and fitting parameters against experimental data. Three experiments were compared, and despite solid single-experiment fits, the cross-validation shows significant problems with generalization of fitted parameters across experiments.

October 13, 2025

Contents

1. Introduction

The mitogen-activated protein kinase/extracellular signal-regulated kinase (MAPK/ERK) pathway and its dynamics play a central role in determining cell fate in response to extracellular inputs. [1] Different cell fates are linked to dynamics of the final node in the cascade, `ERK` kinases in particular. To understand how different dynamic patterns of their behavior arise, a mechanistic model of this pathway was constructed using ordinary differential equations (ODEs). Experimental data was obtained from a series of experiments including fibroblast cells transfected with optogenetic receptor tyrosine kinase (optoRTKs) constructs and an ERK-KTR reporter. The cells were stimulated with different light patterns over the course of each experiment. Model parameters were estimated from this data, and cross-validation techniques were employed to evaluate the generalizability of fitted parameters. Although individual experiments were fitted accurately, the resulting model failed to generalize across conditions, indicating the need for further refinement.

2. Methods & Materials

2.1. Experimental Data

Data used for fitting the model was obtained from an experimental setup consisting of fibroblast cells transfected with an optoEGFR construct (optogenetic actuator) and being stimulated with various patterns of light. Data from 3 experiments were used in our pipeline, representing distinct light activation patterns. All experiments start with a 10 minute period of no stimulation, that was used for calibrating the baseline levels of activity. Sampling rate of each experiment was $\frac{1}{\min}$. Data was prepared by first converting raw intensities captured for nucleus and cytoplasm into a fraction $\frac{I_{\text{cytoplasm}}}{I_{\text{cytoplasm}} + I_{\text{nucleus}}}$ representing active ERK. Baseline subtraction was done on a per-cell level, and afterward normalization was performed for each experimental group separately. First pattern that was investigated was a transient activation pulse for a given amount of time. The experiment was repeated with different durations, namely $t = \{0, 50, 100, 200, 500, 1000\}$ ms. This experiment was used during development for testing and verifying due to its simplicity.
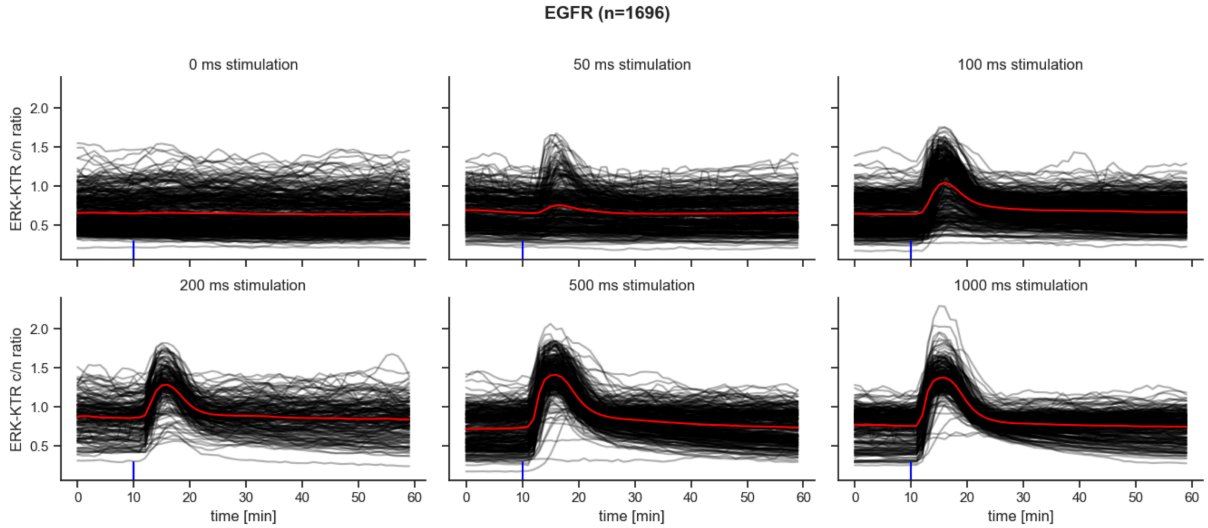

Figure 1: Single cell ERK-KTR activity in transient activation experiment. Each black curve represents a trajectory of a single cell. Red line is a median of all trajectories.

Second pattern that was incorporated was sustained activation. In this experiment, stimulation was started and sustained for a 140 minutes with three different power settings.
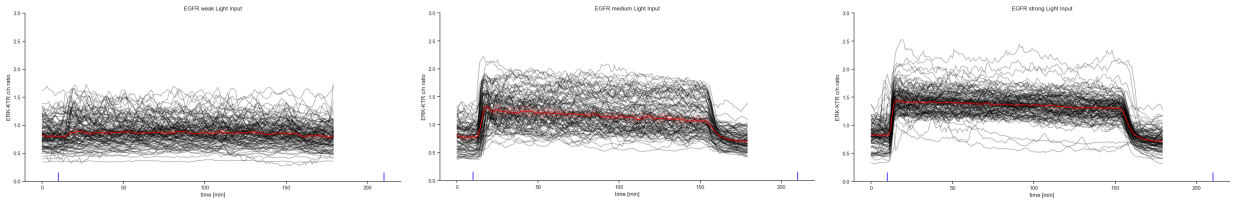

Figure 2: Single cell ERK-KTR activity in sustained activation experiment. Each black curve is a single cell trajectory of ERK-KTR, red line describes median.

Third pattern incorporated into the pipeline was a ramp pattern. This pattern starts by running a light pulse every minute, and increasing the pulse width with every subsequent activation, starting from 0 and ending at 700ms pulse width, resulting in overall ramp shape of the activation curve over time.
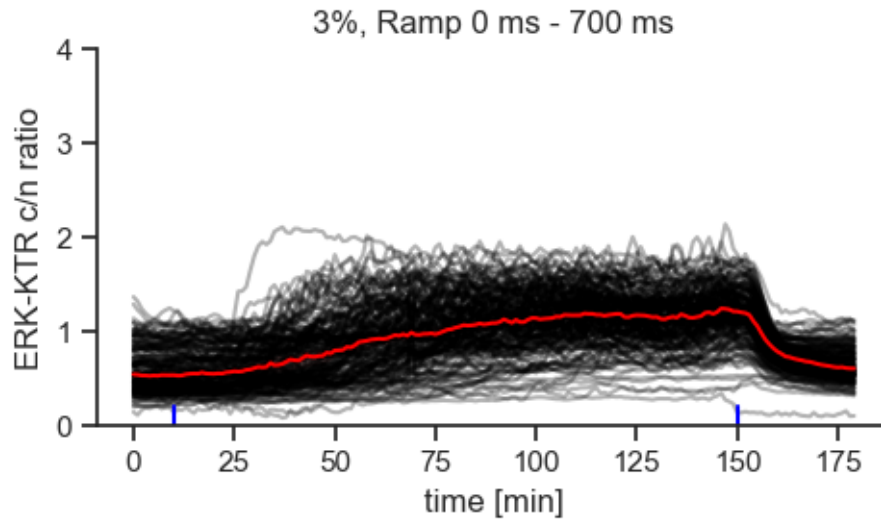
Figure 3: Single cell ERK-KTR activity in ramp activation experiment.
Each black curve is a single cell trajectory of ERK-KTR, red line describes median.

The development and initial testing of modeling pipeline was done using only transient activation experiment. Sustained and Ramp were incorporated as a means of providing cross-validation for the fitting process.

2.2. Model Structure

Finding the balance between simplicity and mechanistic accuracy is the key problem in model definition. Too simple model results in non-relevant findings, since it fails to capture complexity of the problem. Too complex model is harder to operate, and is prone to fragile to complexity explosions, parameter unidentifiability, and poor choice of starting condition leading to nonsensical results.

The chosen model starts at the level of RAS, and does not include the receptor layer. It treats light as a positive term in converting RAS to RAS* (the active form). The standard MAPK/ERK cascade of RAS-RAF-MEK-ERK is preserved. We group whole families of kinases together and represent them as one vertex to preserve ontological grouping while minimizing complexity of the model.

Model also contains a negative feedback loop represented as a separate NFB state variable (Figure 4). Modeling negative feedback as a separate state variable is not mechanistically accurate, but allows for a number of useful properties. It helps with model understandability, as negative feedback has clear and separate parameters that can be tweaked in isolation, while its existence as a state variable in the simulated model helps to track the contribution of negative feedback on the rest of the system. Another remarkable simplification of experimental setup comes from removal of reporter layer (KTR-ERK complex). Presented model assumes that gathered experimental data coming from the reporter is a perfect proxy of actual state of ERK concentration in the cell.
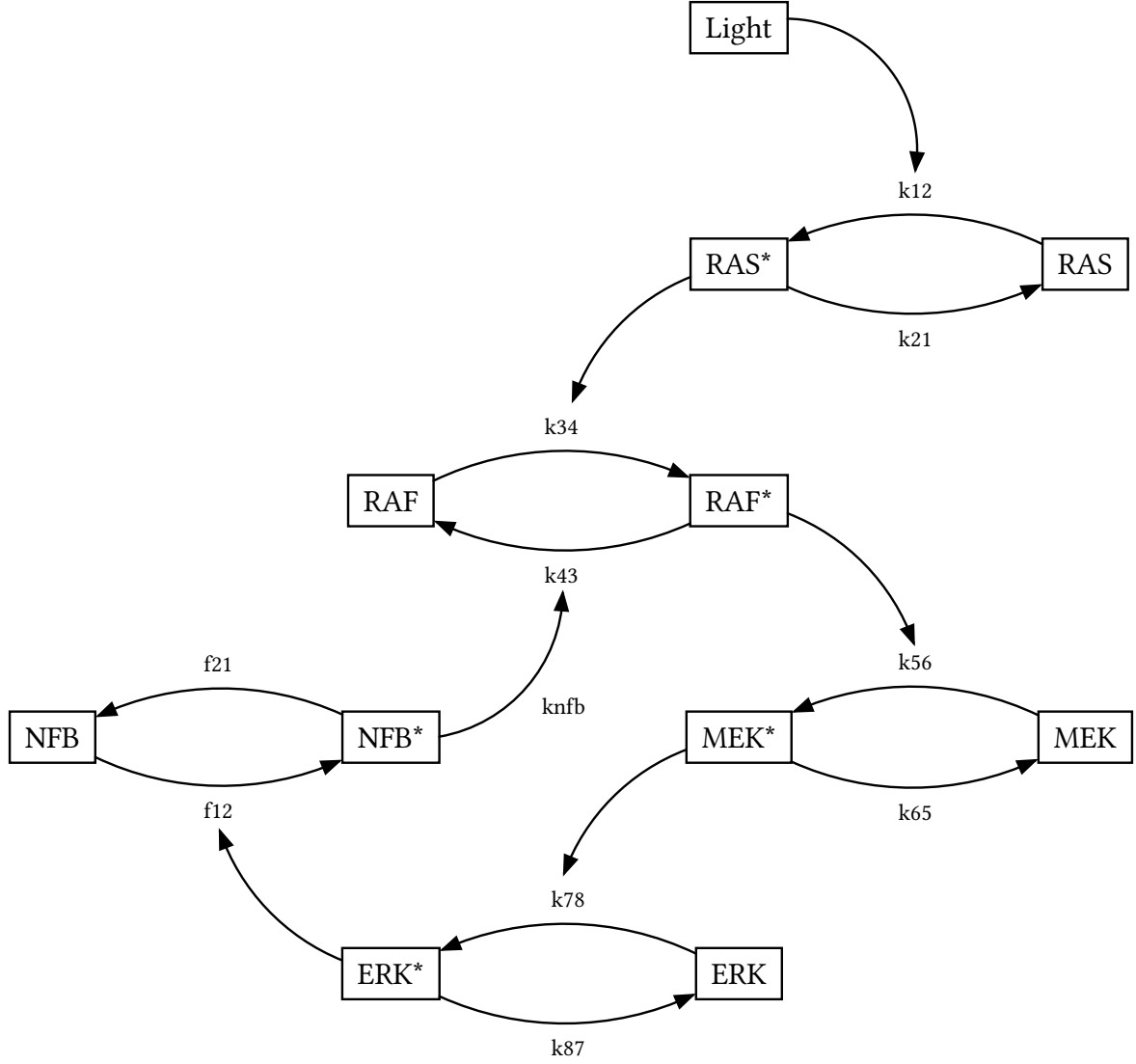
Figure 4: Diagram of the used model, representing simplified MAPK/ERK cascade.

2.3. Ordinary Differential Equations

Ordinary differential equations are a mathematical framework for describing the change of one variable (dependent) over another variable (independent). Its simplest formulation is an expression that equates some mathematical expression to a derivative of our variable in question Y over the independent variable X.

$$\frac{dY(x)}{dX} = f(y(x)) \tag{1}$$

A solution to a differential equation is usually understood as obtaining a $Y(X)$ form, also called a *general solution* [2]. General solutions can be obtained using an analytical solving process, the difficulty of which is heavily dependent on the specific problem being solved. An often encountered problem with analytical solution approach is a problem that contains complex, nonlinearly coupled equations, which do not yield easily to this method. An alternative approach to solving a system that has these characteristics is a numerical one. This method relies on provided initial conditions and Δx resolution to simulate a single trajectory within an ODE system by evaluating the equations sequentially at a consecutive Δx away from the provided starting point. This method, while providing a weaker form of solution, can

deal with harder problems, including those that describe complex, nonlinear systems.

A load-bearing assumptions when picking up an ODEs for modeling dynamics of intracellular concentrations is that within the cell, the system is perfectly mixed (no spatial gradients of concentration occur). This assumption lets us avoid the complexities stemming from tracking chemical gradients within the cell based on position within it, which would be impossible to model using just an ODE system, as multiple additional independent variables arise from having to incorporate positional information.

Basic formulation of our model as a set of differential equations comes down to expressing each family of kinases as a state variable and expressing interactions between these kinases as a positive or negative terms in their respective differential equations.

Variables k and f are parameters of our model: those beginning with k generally concern the cascade, while those beginning with f correspond to the feedback mechanism, with a notable outlier of knfb, which is connected to both.

$$\frac{d\text{RAS*}}{dt} = \text{light} * \left(\frac{\text{RAS}}{K_{12} + \text{RAS}} \right) - k_{21} * \left(\frac{\text{RAS*}}{K_{21} + \text{RAS*}} \right)$$

$$\frac{d\text{RAF*}}{dt} = k_{34} * \text{RAS*} * \left(\frac{\text{RAF}}{K_{34} + \text{RAF}} \right) - (\text{knfb} * \text{NFB*} + k_{43}) * \left(\frac{\text{RAF*}}{K_{43} + \text{RAF*}} \right)$$

$$\frac{d\text{MEK*}}{dt} = k_{56} * \text{RAF*} * \left(\frac{\text{MEK}}{K_{56} + \text{MEK}} \right) - k_{65} * \left(\frac{\text{MEK*}}{K_{65} + \text{MEK*}} \right) \tag{2}$$

$$\frac{d\text{NFB*}}{dt} = f_{12} * \text{ERK*} * \left(\frac{\text{NFB}}{F_{12} + \text{NFB}} \right) - f_{21} * \left(\frac{\text{NFB*}}{F_{21} + \text{NFB*}} \right)$$

$$\frac{d\text{ERK*}}{dt} = k_{78} * \text{MEK*} * \left(\frac{\text{ERK}}{K_{78} + \text{ERK}} \right) - k_{87} * \left(\frac{\text{ERK*}}{K_{87} + \text{ERK*}} \right)$$

Figure 5: System of ODEs governing the simplified MAPK/ERK cascade.

The final assumption held was that on the timescale of observed experiments, the total amount of active and inactive form of a given molecule is constant (a "conserved moieties" assumption). Such assumption allows for description of entire model using only half of the state variables, by introducing each sum of forms as a constant in our model, thereby allowing us to refer the concentrations of active and inactive parts using a single concentration and a total (for example, instead of using RAS* and RAS, we can use RAS* and $\text{RAS}_{\text{total}} - \text{RAS*}$). This operation makes the simulation less computationally complex [2]. Since the data was already normalized to account for varying cell size (removing baseline and scaling by max magnitude per group) for active ERK fraction, total kinase concentration was set to a constant of 1.

2.4. Modeling & Simulation pipeline

Model definition was done in symbolic form using SymPy in python [3], as a list of symbolic differential equations. The same tool was also used to lower the symbolic expression down to a numerical representation (`lambdify` function). A constructed model consists of a set of differential equations and parameter values. An effort was made to make this pipeline model-and-experiment agnostic and have low friction for implementing new models. This effort led to an architecture where each new model needs only to fulfill a simple interface for defining

its equations and parameters, and each new experiment needs to define its own pattern of input and a parsing function for the data it generated.

An interactive environment for simulating behavior and exploring perturbations to parameters was constructed using marimo notebooks.

Parameter estimation was done using tools from SciPy library [4], namely `minimize` and `solve_ivp` to optimize loss function and to solve a numerical system respectively. The general scheme involved minimizing residual sum of squares for the data given in an experiment across all the groups in a given experiment.

Codebase was structured around a `Model` class that implements model definition, parameter estimation and simulating a trajectory given a stimulation pattern, parameters, and the initial condition. Each experiment has its own light-stimulation function and a function to read, filter, and normalize data.

Thus, to incorporate a new experiment into the model, one has to only implement `light_fn` and some kind of function that will parse and return correctly shaped pd.dataframe object as experimental data. Convention here was to have 3 columns: `time`, `group`, and `y`. Additional columns can be incorporated, however `group` values must be unique across experiments.

Functionality to provide alternative models was also implemented: all models need to supply a `model_definition` function that provides symbolic differential equations, and a list of parameters, constants and state variables.

During development, simulation tool was used to 'hand-pick' a solid starting points for parameter initial values, however during model validation, all training runs started with the same parameter set randomly sampled from a uniform distribution $\mathbb{U}_{[0,2]}$.

3. Results

3.1. Parameter estimation from a single experiment

The preliminary fits over single experiments captures each individual dynamic response quite well in the broad strokes. However, a noticeable pattern across these peaks is that the model rarely captures quantitative metrics such a $c_{\max}$, cannot account for changes in baseline, and has trouble accurately fitting scenarios with wide range of stimulation conditions.
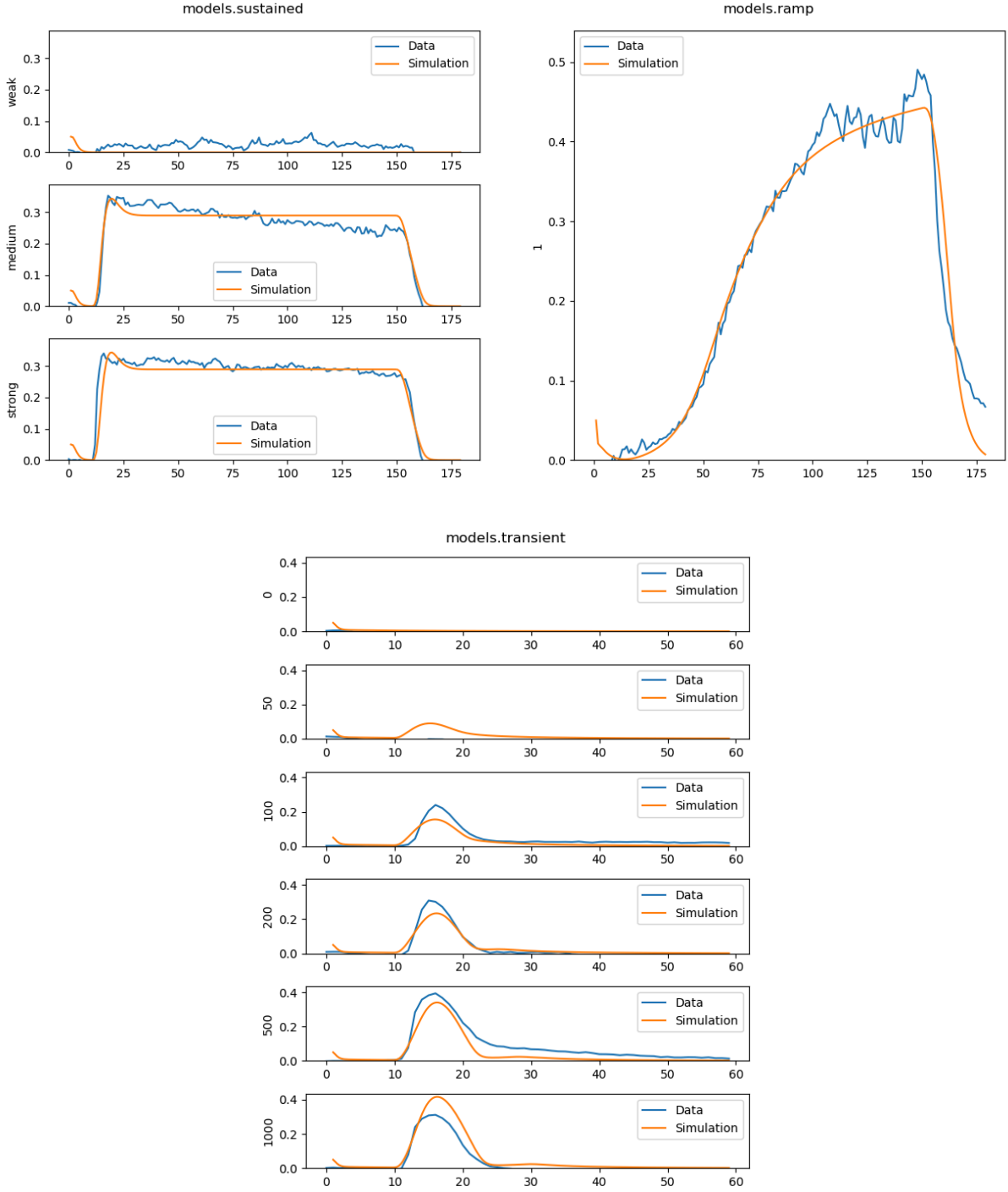

Figure 6: Results of 3 single-experiment fits. X axis shows time (min), and Y axis shows normalized cytoplasmic ERK-KTR intensity, representing active ERK fraction. Label next to Y axis denotes experimental group.
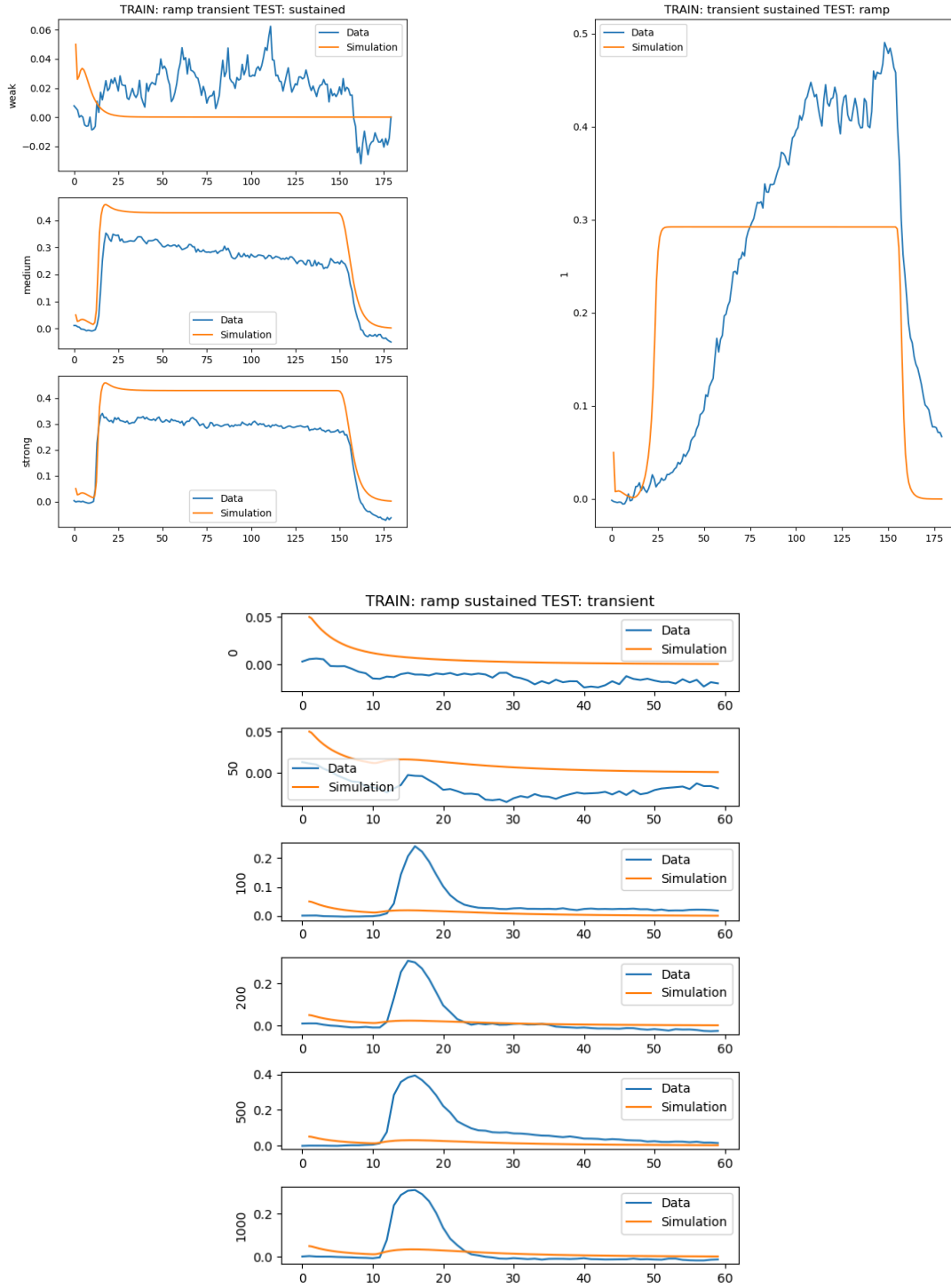
3.2. Cross-validation

Figure 7: Results of 3-fold cross validation. X axis shows time (min), and Y axis shows normalized cytoplasmic ERK-KTR intensity, representing active ERK fraction. Label next to Y axis denotes experimental group. There is observable lack of generalization between experiments. Model trained on transient and ramp experiments and tested on sustained shows the best results in that it reproduces the shape of the activation we see in the data. However, the quantitative values outputted by the model are consistently overshooting the experimental observations. Other folds of cross-validation fail to reproduce the ERK activation dynamics at all.

Cross-validation was performed to evaluate the generalizability of parameter sets fitted on one experiment when applied to others (Figure 7). Significant variation in predictive accuracy was observed across validation folds. The model trained on the transient and ramp activation datasets and tested on the sustained experiment exhibited the highest degree of qualitative agreement, correctly reproducing the overall shape of the activation curve. However, the model consistently overestimated activation magnitudes and failed to accurately capture the saturation plateau observed in the experimental data.

In contrast, parameter sets trained on the sustained or ramp experiments failed to reproduce ERK activation patterns in the transient experiment, producing responses that were temporally misaligned and quantitatively inconsistent. This poor cross-experimental transfer indicates that fitted parameters are highly context-dependent and may be influenced by experimental conditions such as stimulation pattern, sampling frequency, and cellular heterogeneity.

The results therefore demonstrate that the current model lacks global parameter robustness and cannot yet serve as a unified predictor of ERK activation dynamics across distinct stimulation regimes. The cause is not certain, but both a sub-optimal model architecture and a lack of sophistication in training regiment could be interesting targets for improvement.

4. Discussion

4.1. Time resolution limitations

During implementation of the parameter estimation regime, a technical difficulty was encountered. The experiments had been replicated multiple times with different parameter values for light stimulation, usually differing in stimulation time of a pulse of light, with values ranging from 50ms to 2000ms. At the same time, data for those experiments was collected with a rate of one sample per minute. Such difference in time ranges between sampling and input means that our experimental data will never be able to differentiate between the light stimulation duration groups within an experiment just by looking at the data (we would need to increase the sampling rate 1200 times to be able to discern signals that lasted 50ms, the most fine-grained light signal in our experimental data). To circumvent this problem, two solutions were contemplated.

1. An interpolation algorithm could have been used to synthetically create data points of the sampling rate we desire. This forces our new data points to inherit our assumptions about how the data is interpolated, which could introduce a systematic bias (as example, for linearity).
2. A proxy metric for a total light energy of a light pulse for a datapoint is introduced instead of a "binary" baseline. This allows for more flexibility but at a cost of having to create a realistically-scaling function that works for all kinds of experiments and across different levels of magnitude of light stimulation duration.

After theoretical evaluation of pros and cons of both, a second solution strategy was picked, due to a better compatibility with the goal of having short training times. Despite dealing with the hurdle at hand and enabling further steps, this resolution creates its own problems. With each experiment we add to our roster, one needs to manually implement its corresponding light-stimulation function, and what's more important, one also needs to make sure the light functions from different experiments are compatible with each other - a consistent formula for translating between experimental setup and computational representation is important to establish.

4.2. Parameter identifiability and model robustness

The limited generalizability of the model likely reflects issues of parameter identifiability - a concept where even when a model accurately reproduces individual experimental datasets, its parameters can not be uniquely determined [5].

This arises from strong correlations between parameters that produce elongated, flat regions in the residual landscape - making it harder for fitting algorithm to traverse and find optimal solution.

Only a few parameter combinations ("stiff directions") are well constrained by the data, while the majority ("sloppy directions") remain weakly identifiable. Consequently, optimization may converge to different parameter values without affecting model fit quality.

Improved identifiability could be achieved through joint fitting across many experiments, inclusion of prior information, and experimental designs that specifically perturb correlated reactions.

5. Future work

Future work should focus on improving both the robustness and applicability of the modeling framework. A global optimization stage should be introduced prior to local parameter fitting to ensure broader exploration of the parameter space and to reduce the risk of convergence to local minima. The modeling framework should also be extended to support multiple, interchangeable model structures, enabling systematic comparison of competing hypotheses and quantification of their relative explanatory power. Comprehensive sensitivity analyses will be required to identify parameters that most strongly influence system behavior and to guide model refinement. Ultimately, the developed model and accompanying optimization tools could be integrated into an automated experiment design pipeline, allowing for iterative selection of experimental conditions and stimulation patterns that maximize information gain and minimize parameter uncertainty. Additionally, tighter integration with the experimental setup — particularly through improved and standardized generation of light-stimulation functions for each experiment could further enhance model fidelity.

Bibliography

[1] H. Ryu *et al.*, "Frequency modulation of ERK activation dynamics rewires cell fate," *Molecular Systems Biology*, vol. 11, no. 11, Nov. 2015, doi: 10.15252/msb.20156458°.

[2] D. Fey, M. Dobrzyński, and B. N. Kholodenko, "Modeling with Ordinary Differential Equations," *Quantitative Biology: Theory, Computational Methods, and Models*. MIT Press, 2018.

[3] A. Meurer *et al.*, "SymPy: symbolic computing in Python," *PeerJ Computer Science*, vol. 3, p. e103, Jan. 2017, doi: 10.7717/peerj-cs.103°.

[4] P. Virtanen *et al.*, "SciPy 1.0: Fundamental Algorithms for Scientific Computing in Python," *Nature Methods*, vol. 17, pp. 261–272, 2020, doi: 10.1038/s41592-019-0686-2°.

[5] B. C. Daniels, M. Dobrzyński, and D. Fey, "Parameter Estimation, Sloppiness, and Model Identifiability," *Quantitative Biology: Theory, Computational Methods, and Models*. MIT Press, 2018.

Index of Figures